© 2015. Published by The Company of Biologists Ltd | Development (2015) 142, 743-752 doi:10.1242/dev.114629

RESEARCH ARTICLE

Cavefish eye loss in response to an early block in retinal differentiation progression

Manuel Stemmer[1,‡], Laura-Nadine Schuhmacher[1,*,‡], Nicholas S. Foulkes[1,2], Cristiano Bertolucci[3] and Joachim Wittbrodt[1,§]

ABSTRACT

The troglomorphic phenotype shared by diverse cave-dwelling animals is regarded as a classical example of convergent evolution. One unresolved question is whether the characteristic eye loss in diverse cave species is based on interference with the same genetic program. *Phreatichthys andruzzii*, a Somalian cavefish, has evolved under constant conditions in complete darkness and shows severe troglomorphic characteristics, such as complete loss of eyes, pigments and scales. During early embryonic development, a complete eye is formed but is subsequently lost. In *Astyanax mexicanus*, another blind cavefish, eye loss has been attributed to interference during eye field patterning. To address whether similar pathways have been targeted by evolution independently, we investigated the retinal development of *P. andruzzii*, studying the expression of marker genes involved in eye patterning, morphogenesis, differentiation and maintenance. In contrast to *Astyanax*, patterning of the eye field and evagination of the optic vesicles proceeds without obvious deviation. However, the subsequent differentiation of retinal cell types is arrested during generation of the first-born cell type, retinal ganglion cells, which also fail to project correctly to the optic tectum. Eye degeneration in both species is driven by progressive apoptosis. However, it is retinal apoptosis in *Phreatichthys* that progresses in a wave-like manner and eliminates progenitor cells that fail to differentiate, in contrast to *Astyanax*, where lens apoptosis appears to serve as a driving force. Thus, evolution has targeted late retinal differentiation events, indicating that there are several ways to discontinue the development and maintenance of an eye.

KEY WORDS: *Astyanax mexicanus*, Retinal development, Evolution, Eye morphogenesis, *Phreatichthys andruzzii*, Troglomorphism

INTRODUCTION

Cave inhabitants often share characteristic changes in morphology termed troglomorphisms (Pipan and Culver, 2012). These changes result from the absence of light and have been commonly separated into regressive and constructive traits (Hecht et al., 1988). Regressive traits are characterised by the loss of an organ or function, whereas constructive traits lead to an increase in the number or performance of an organ. The most prominent regressive traits in cavefish are eye and pigment loss (Hecht et al., 1988; Jeffery, 2001). Cave species often form an embryonic eye that apparently develops normally before it degenerates during juvenile or early adult stages, in most cases without ever being functional (Berti et al., 2001; Besharse and Brandon, 1974; Hecht et al., 1988). One hypothesis is that neutral mutations accumulate in eye-specific genes after loss of the evolutionary pressure to retain visual perception due to the constantly dark environment (Pipan and Culver, 2012; Wilkens, 2011). However, it has recently been suggested that in some cases eye loss might occur by the selection of a gene that has positive effects on unrelated features, thus increasing the organism's fitness via pleiotropic effects (Protas and Jeffery, 2012; Rohner et al., 2013; Yamamoto et al., 2009). Eye degeneration occurs in several cavefish species (Berti et al., 2001; Meng et al., 2013; Wilkens, 2007), of which *Astyanax mexicanus* is the best studied (Alunni et al., 2007; Hinaux et al., 2011; Jeffery, 2009; Rétaux et al., 2008; Strickler et al., 2007; Yamamoto, 2000). In this species, decisions for later eye degeneration are apparently rendered during patterning of the early eye field (Menuet et al., 2007; Pottin et al., 2011; Yamamoto et al., 2004). A key, unresolved question is whether this mechanism of eye loss is conserved in other, unrelated cavefish species. To address this issue, we have studied in detail the eye development of *Phreatichthys andruzzii*, a blind cave-dwelling cyprinid that exhibits an even more severe troglomorphic phenotype.

P. andruzzii has recently been introduced as a cavefish model due to its extreme troglomorphism (Cavallari et al., 2011). The wild population, sampled in the Bud-Bud region of Somalia in a sub-Saharan horizontal limestone formation, has been isolated in a cave environment for approximately two million years. The adult fish completely lack pigment and eyes, as well as scales. Conversely, the number of neuromast sensory cells is dramatically increased (Berti et al., 2001; Dezfuli et al., 2009a,b). The eyes in *Phreatichthys* develop initially, but then degenerate and are eventually overgrown by orbit tissue and skin (Berti et al., 2001). The eye does not exhibit any functional architecture at any time point.

It has been shown that the vertebrate eye develops along an evolutionarily conserved spatiotemporal axis, with respect to morphogenesis and the expression of corresponding key transcription factors (Agathocleous and Harris, 2009; Kay et al., 2005; Loosli et al., 2001; Zuber et al., 2003). Eye formation is initiated by the activity of conserved transcription factors (Six3, Sox2, Pax6, Rx3), with the specification of the eye field in the anterior neuroectoderm. The eye becomes obvious with the lateral evagination of the optic vesicle (Shh/Gli, Rx3) and subsequent optic cup formation (Pax2, Pax6), followed by growth (Rx2, Sox2). These events are all tightly connected to changes in the expression of the above-mentioned (transcription) factors.

Growth and morphogenesis are tightly interconnected with the stepwise and highly stereotypic differentiation of retinal cell types. Initially undifferentiated retinal progenitor cells differentiate into

[1]Centre for Organismal Studies (COS), Heidelberg University, Heidelberg 69120, Germany. [2]Institute of Toxicology and Genetics (ITG), Karlsruhe Institute of Technology, Karlsruhe 76131, Germany. [3]Department of Life Sciences and Biotechnology, University of Ferrara, Ferrara 44121, Italy.
*Present address: Department of Pharmacology, Cambridge University, Cambridge CB2 3DY, UK.
‡These authors contributed equally to this work

§Author for correspondence (jochen.wittbrodt@cos.uni-heidelberg.de)

Received 20 June 2014; Accepted 15 December 2014

Development (2015) 142, 743-752 doi:10.1242/dev.114629

the seven distinct cell types of the adult retina in tightly coordinated temporal progression: retinal ganglion cells (RGCs) are born first, followed by horizontal, amacrine and bipolar cells and the late-born rod and cone photoreceptors, as well as non-neuronal Müller glia cells (Centanin and Wittbrodt, 2014). The tip of the retina, an area called the ciliary marginal zone (CMZ), remains undifferentiated and functions as a stem cell niche, contributing to the life-long growth of the eye (Centanin et al., 2011).

We found that in *Phreatichthys* the establishment of the eye field and the initial steps of retinal morphogenesis appear largely normal, as indicated by the expression of transcription factors involved in the corresponding steps. These genes are expressed in patterns highly reminiscent to those described for other teleosts. Conversely, markers for RGCs are expressed only partially and genes involved in the differentiation of subsequently formed cell types were not expressed or only at very low levels. In addition to our *in situ* hybridisation study, we observed disorganisation of the retinal architecture and strong activity of the apoptosis gene encoding Caspase3, an indicator of cell death.

RESULTS

Experimental approach

In order to investigate early retinal development in *P. andruzzii*, we documented the expression of key marker genes selected for their involvement in retinal development and performed *in situ* hybridisation to assay and correlate their expression with morphologically apparent alterations. Early eye field specification, stem cells and retinal progenitor cells (RPCs) were visualised using probes detecting *six3a*, *pax2.1*, *pax6a*, *sox2*, *rx3* and *rx2* transcripts. Embryonic midline signalling was analysed with probes against *shh*, *nkx2.1* and *fgf8*. As specific markers for RPCs at later stages, *six3* and *nr2e1* were selected.

Differentiated cell types in the retina were identified by the expression of well-established cell type-specific transcription factors. In particular, we analysed *atoh7*, a transiently expressed transcription factor that marks the genesis of RGCs (Kay et al., 2001). These cells were additionally visualised by *pou4f2* and *ils1* expression (Moshiri et al., 2008; Mu et al., 2008). Photoreceptors were analysed by the expression of *crx*, *opsin* (long-wave sensitive) and *rhodopsin*. *barhl2* (Jusuf et al., 2012) was employed as an amacrine cell marker and *vsx1* (Passini et al., 1997) as a marker for bipolar cells. As none of these genes had been described for *Phreatichthys* so far, we cloned and sequence validated all of the respective orthologues from *Phreatichthys* cDNA.

During the development of *Phreatichthys*, the retina started to degenerate rapidly after 45 h post fertilisation (hpf). Just 10 hours later, the eyes were strikingly small or barely visible and started to sink into the surrounding tissue. We thus focused our detailed analysis on the first 45 h of development, divided into six developmental stages: 10 hpf, 19/20 hpf, 31 hpf, 35 hpf, 38 hpf and 45 hpf.

Early patterning and eye morphogenesis

To examine the early phase of eye field patterning, optic vesicle morphogenesis and optic cup formation, we analysed the expression of *sox2*, *six3a*, *rx3*, *rx2*, *pax2.1* and *pax6a*. To address embryonic midline signalling, we used probes against *fgf8*, *shh* and *nkx2.1*.

The pan-neural marker gene *sox2* promotes neural fate, maintains progenitor cells in an undifferentiated state and is additionally active in promoting stemness in adult stem cells (Agathocleous et al., 2009; Ekonomou et al., 2005). In *Phreatichthys* embryos, early expression of *sox2* was detected throughout the neuroectoderm, including the eye field (10 hpf) and optic vesicles (19 hpf) (Fig. 1A,B). *six3a* is one of the initiation factors for eye development (Carl et al., 2002; Loosli et al., 1999) and was detected early in the forming eye field (Fig. 1C). It was also expressed in the developing forebrain of *P. andruzzii* at 19 hpf (Fig. 1D).

Retinal homeobox (*rx*) genes represent a set of key factors involved in vertebrate eye patterning and morphogenesis. Loss of function of some of these genes leads to eyeless phenotypes in mouse and fish (Loosli et al., 2001, 2003; Mathers et al., 1997). The role of Rx3 is to guide cells through optic vesicle evagination towards a photoreceptor fate in the late gastrula, while Rx2 is suggested to function in photoreceptors and in actively proliferating retinal stem and progenitor as well as Müller glia cells.

Transcripts of *rx3* were detected in the anterior neuroectoderm (eye field) at 10 hpf and the optic vesicles and midbrain at 19 hpf (Fig. 1E,F). At 31 hpf, staining for both *sox2* and *rx2* was strong in the newly formed retina, where it was confined to the periphery (supplementary material Fig. S1E,H), consistent with their expression in the forming CMZ in other teleost species.

In *Astyanax*, an early expansion of midline signalling, highlighted by the expression of the secreted signalling factor Shh, has been proposed to contribute to the subsequent eye loss (Menuet et al., 2007; Yamamoto et al., 2004). In response, *fgf8* is expressed earlier in the *Astyanax* cavefish than in its surface counterpart (Pottin et al., 2011). We therefore analysed *Phreatichthys fgf8* and *shh* expression. We detected apparently normal *fgf8* expression in *Phreatichthys* embryos, as well as *fgf8* transcripts initially in the anterior neuroectoderm and at the midbrain-hindbrain boundary (MHB) (10 hpf, Fig. 1G). At subsequent stages, we found *fgf8* expression in the anterior midline as well as the MHB (20 hpf, Fig. 1P). Also, the *shh* expression pattern appeared unaffected and it was expressed along the embryonic midline at 10 hpf (Fig. 1I) and in the ventral neural tube and notochord at 19 hpf (Fig. 1J). Consequently, the expression pattern of the *shh* downstream target gene *nkx2.1* is indistinguishable from the pattern at comparable stages in other teleost species (Fig. 1K,L).

Fates along the mediolateral axis of the neural plate are highly sensitive to Shh signalling. We addressed whether Shh signalling in the ventral midline affects the establishment of proximal or distal retinal fates, indicative of altered Shh signalling activity (Macdonald et al., 1995). We thus compared the complementary expression domains of proximal (Pax2) and distal (Pax6) markers.

In the eye field (10 hpf), we detected *pax2* expression in the proximal eye field adjacent to midline *shh* (compare Fig. 1I with 1M). As development proceeded, *pax2* expression remained confined to the proximal part of the evaginated optic vesicle (Fig. 1N) and was clearly excluded from the distal domain of the forming optic vesicle (Fig. 1N, arrow).

Initial *pax6* expression demarcates the early eye field. Here, it plays a key role in the formation of the optic primordia and subsequently in the promotion of progenitor cell proliferation (Lagutin et al., 2003; Walther and Gruss, 1991; Zaghloul and Moody, 2007). At 10 hpf (early neurula) *pax6* mRNA was detected in the eye field of the anterior neuroectoderm and the forming dorsal diencephalon (Fig. 1O). At 19 hpf (optic vesicle stage) the eye field expression of *pax6* was shifted distally to the RPCs of the evaginating optic vesicles (Fig. 1P) and, at a later stage (31 hpf), its expression had spread throughout the retina (supplementary material Fig. S1A,B). We also studied the pattern of the distally expressed key retinal gene *pax6* as well as of markers for the distalmost domain of the retina, the CMZ, at subsequent stages of retinal development. *pax6* expression was detected in a layer close

Development (2015) 142, 743-752 doi:10.1242/dev.114629

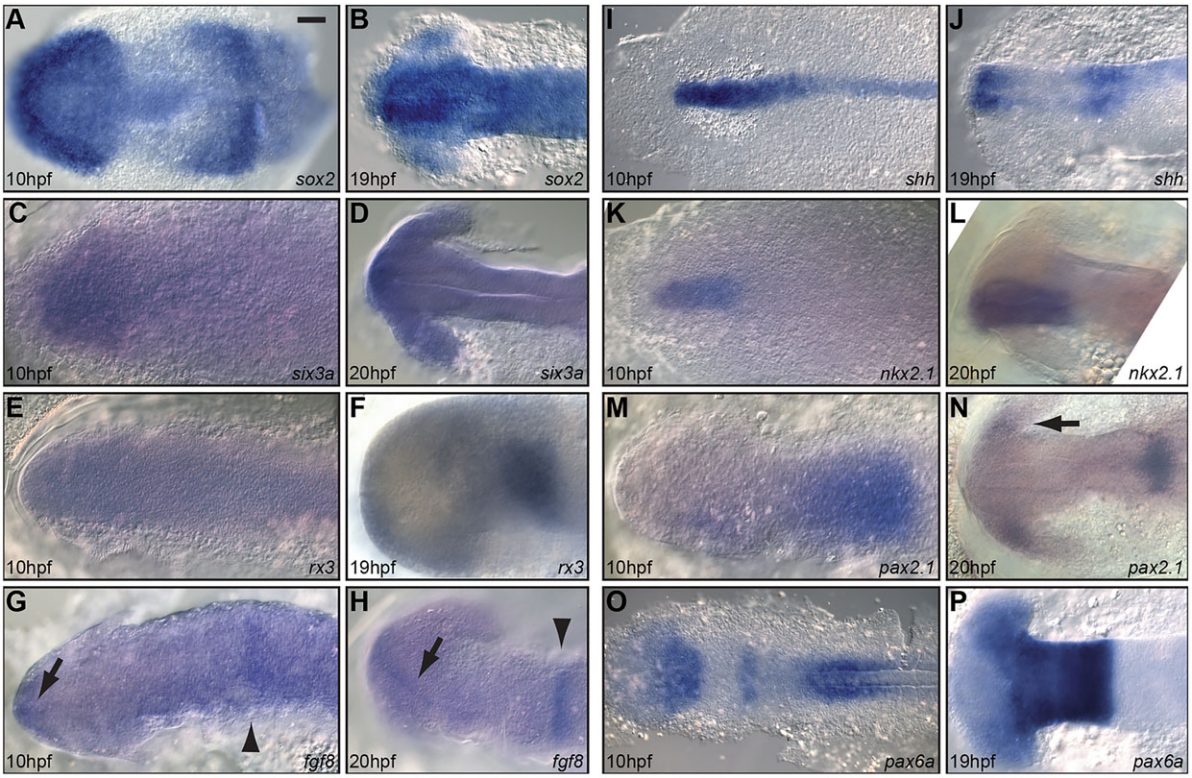

Fig. 1. Early patterning and eye morphogenesis in *Phreatichthys andruzzii*. *In situ* hybridisation with antisense RNA probes, stained with visible dye NBT/BCIP. Stages 10 hpf and 19/20 hpf show dorsal views of embryos dissected from yolk, anterior to the left. *sox2* staining was present throughout the entire neuroectoderm at 10 hpf (A) and in brain and optic vesicles at 19 hpf (B). *six3a* was expressed in the eye field at 10 hpf (C) and in the anterior neuroectoderm and optic vesicles at 20 hpf (D). *rx3* was expressed throughout the entire anterior neuroectoderm at 10 hpf (E) and in the evaginating optic vesicles and forebrain at 19 hpf (F). *fgf8* was detected rostrally in the embryonic midline at 10 hpf (G) and extending posteriorly at 20 hpf (H) (arrows) and in the MHB (arrowheads). *shh* was expressed along the midline at 10 hpf (I) and 19 hpf (J), markedly in the ventral forebrain and midbrain. *nkx2.1* was expressed in the anterior midline, similar to *shh* at 10 hpf (K) and forebrain at 20 hpf (L). *pax2.1* was expressed in the MHB at 10 hpf and 20 hpf (M,N) and optic stalk at 20 hpf (N, arrow). *pax6* was expressed in the eye field, midbrain and hindbrain at 10 hpf (O). At 19 hpf (P), *pax6* expression was additionally seen in the evaginating optic vesicles. Scale bar: 50 µm.

to the lens (Fig. 2A; supplementary material Fig. S1A-D), consistent with its expression in RGCs as reported in other teleosts. Similarly, we detected very faint *six3* expression throughout the entire retina (Fig. 2E; supplementary material Fig. S1L-N), consistent with proper proximodistal pattering of the early eye field. The expression of *rx2* and *sox2* in the periphery of the retina hints at the establishment of a CMZ (Centanin et al., 2011), which is the stem cell domain of anamniotes that contributes to life-long growth of their retina (Fig. 2B-D; supplementary material Fig. S1E-K). The formation of an active CMZ is further supported by PCNA immunohistochemistry revealing active proliferation in this domain (Fig. 2G,G′). In contrast to other teleosts however, the nuclear receptor *nr2e1* (*tlx*) was only weakly expressed here (Fig. 2F; supplementary material Fig. S1).

Our data indicate that there is no apparent enhancement or absence of the expression of key genes involved in the establishment

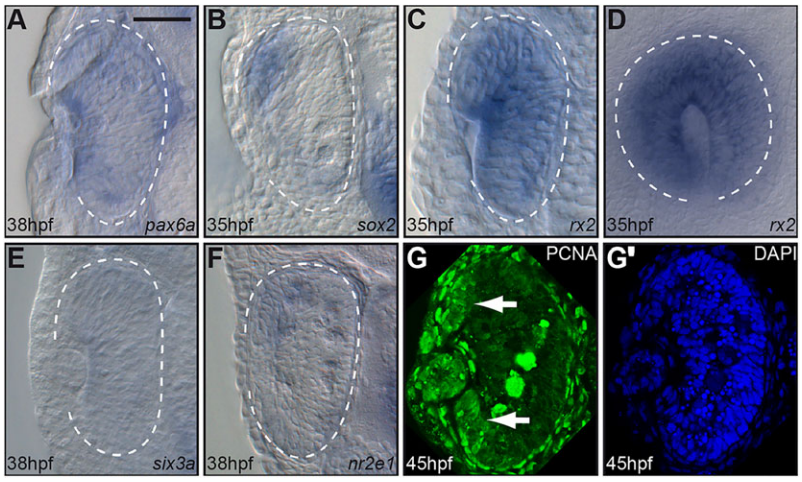

Fig. 2. Establishing the CMZ in *P. andruzzii*. *pax6*, *sox2* and *rx2* were prominently expressed in the retina at 35-38 hpf (A-D). *pax6* was expressed throughout the retina, slightly stronger closer to the lens (A). *sox2* expression at 35 hpf was confined to a dorsal peripheral part of the retina (B). *rx2* expression was strong across the retina (C); a lateral view shows *rx2* expression forming a ring around the lens (D). Weak *six3a* expression was observed at 38 hpf (E). Low-level *nr2e1* expression was observed in the dorsal peripheral part at 38 hpf (F), reminiscent of *sox2*. Transverse sections (A-C,E,F) and lateral view (D), dorsal up. Anti-PCNA immunohistochemistry revealed signal in the CMZ region at 45 hpf (G, arrows); DAPI channel is shown in G′. Retinae are encircled by dashed lines. Further stages are shown in supplementary material Fig. S1. Scale bar: 50 µm.

Development (2015) 142, 743-752 doi:10.1242/dev.114629

of the eye field, its subsequent patterning and optic vesicle evagination. Apparently, the levels of midline signalling do not repress distal retinal fates in *Phreatichthys* and a CMZ is initially established. We therefore extended our analysis to later stages and specifically investigated genes involved in the differentiation of retinal cell types and the layering of the retina.

Differentiation and layering of the retina does not proceed in *Phreatichthys*

In all vertebrates, retinal cell types are born in a stereotypic temporal order resulting in a clear retinal lamination. RGCs are formed first, followed by cone photoreceptors, amacrine and horizontal cells and eventually bipolar cells, rod photoreceptors and Müller glia cells (Centanin and Wittbrodt, 2014). In zebrafish, the initial wave of retinal differentiation giving rise to RGCs is preceded by a central-to-peripheral spreading of *atoh7* expression in the retina (Kay et al., 2005). In the absence of Atoh7, RGCs cannot differentiate from RPCs. We used *atoh7* as a marker for the initiation of RGC differentiation and detected its initial expression in a central area of the *Phreatichthys* retina at 31 hpf (Fig. 3A), from where, as in zebrafish, *atoh7* expression spreads towards the periphery at 35 hpf as an expanding ring (Fig. 3B), similar to the expression of *rx2* (Fig. 2C,D). Independently of *atoh7*, *isl1* expression marks RGCs, but in a differentiated state. *isl1* followed *atoh7* expression from the centre (35 hpf, Fig. 3F) to the periphery (38 hpf, Fig. 3G) and was expressed in a ring domain directly adjacent to the lens at 38 hpf

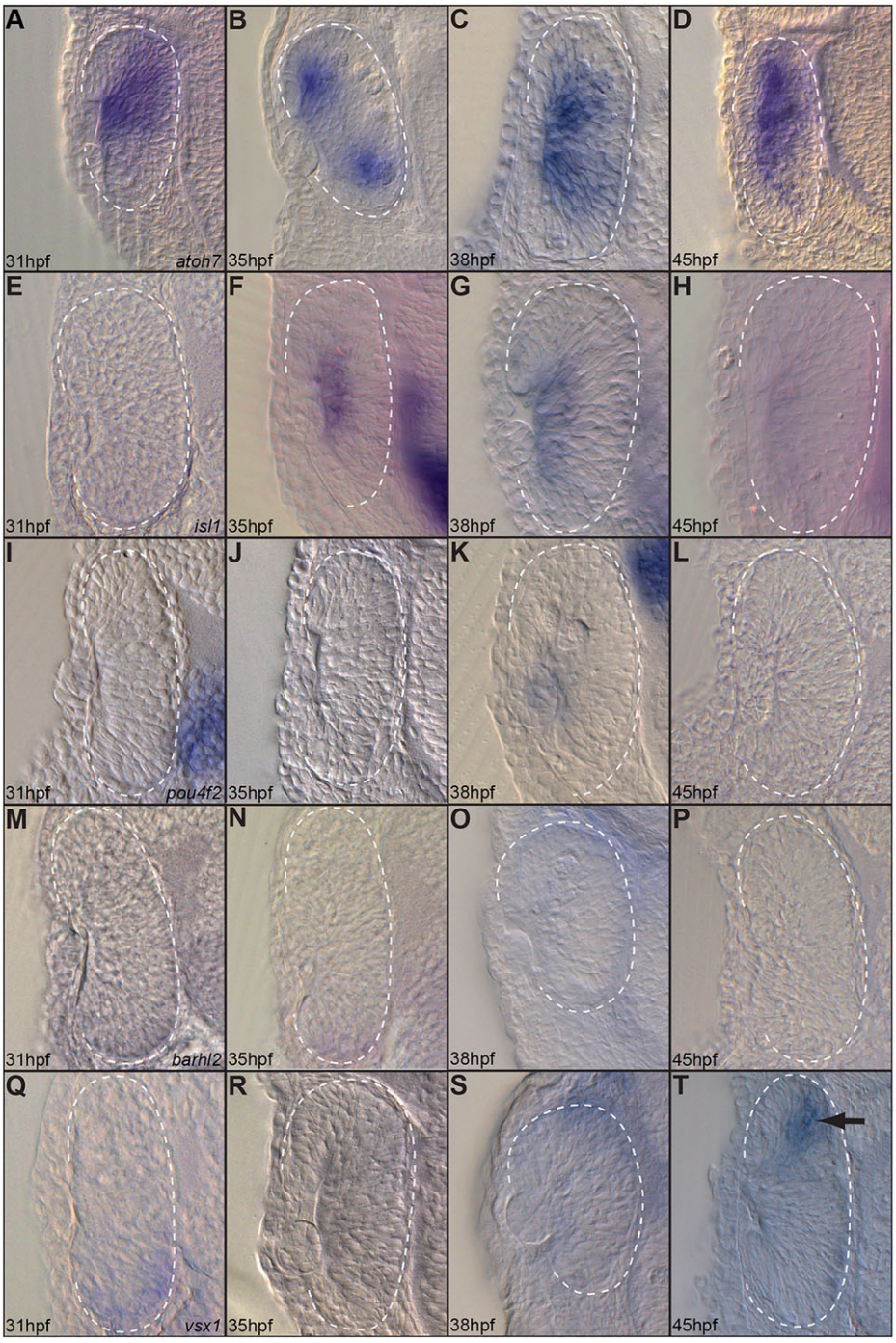

Fig. 3. Expression of differentiation markers in the retina of *P. andruzzii*. *atoh7* (differentiating RGCs) was expressed centrally in the retina at 31 hpf (A) and spread towards the periphery at 45 hpf (B). At 38 hpf (C) and 45 hpf (D) expression remained strong. Adjacent to the lens, *isl1* (differentiated RGCs) follows the *atoh7* expression pattern from the centre (35 hpf, F) to the periphery (38 hpf, G). At 31 hpf (E), no *isl1* expression was detectable yet. At 45 hpf (H), *isl1* expression was reduced markedly. *pou4f2* (differentiated RGCs) was detected only faintly from 31-38 hpf (J,K) close to the lens (RGC region) and was not detectable at 31 hpf (I) and 45 hpf (L). The amacrine cell marker *barhl2* was not expressed at any of the stages analysed (M-P). (Q-T) *vsx1* (bipolar cell marker) showed ectopic staining at various time points: 31 hpf (Q), 38 hpf (S) and 45 hpf (T, arrow). Retinae are encircled by dashed lines. All images show transverse sections.

Development (2015) 142, 743-752 doi:10.1242/dev.114629

(Fig. 3G). In contrast to its expression in zebrafish, *isl1* expression was strongly reduced at subsequent stages (Fig. 3H). As a third marker for terminally differentiated RGCs we employed *pou4f2*. It was faintly expressed from 31 hpf to 38 hpf close to the lens, which is where differentiated RGCs are located in a functional retina (Fig. 3I-K). Similar to *isl1*, the expression of *pou4f2* was barely detectable beyond 40 hpf (Fig. 3L). Taken together, these results indicate that RGCs are initially formed but not maintained as fully differentiated cells. Whereas the expression of *atoh7*, which is a marker for cells in their final mitosis prior to RGC differentiation, is maintained beyond 45 hpf, the expression of the terminal differentiation markers *isl1* and *pou4f2* ceases (Fig. 3D,H,L).

Although present in the genome, no expression of photoreceptor marker genes (*crx*, *opsin*, *rhodopsin*) was detectable by whole-mount *in situ* hybridisation or RT-PCR (data not shown). To address the presence of the subsequent cell types born in the vertebrate retina, we analysed the expression of *barhl2* (amacrine cells) and *vsx1* (bipolar cells).

barhl2 was not expressed at any of the stages examined (31-45 hpf, Fig. 3M-P). This was also partially the case for the bipolar cell marker *vsx1*, which showed occasional transient expression in small patches randomly located in the neuroretina (Fig. 3Q-T). In the absence of apparent RGC and photoreceptor differentiation and retinal lamination, a faint *vsx1* staining could be observed at 31 hpf in the ventral retina (Fig. 3Q), at 38 hpf at the dorsal edge of the retina (Fig. 3S), and around a rosette structure indicative of apoptotic centres at 45 hpf (Fig. 3T, arrow).

Taken together, these data indicate that RGCs are born in the retina and their differentiation is initiated but not maintained. Strikingly, no differentiation of any of the subsequently born cell types could be detected with multiple independent markers.

Ganglion cell projections to the tectum are impaired in *Phreatichthys*

To address whether mature RGCs with fully extended axons were formed and whether these project to the optic tectum, we visualised the axonal tracts in the nervous system of *Phreatichthys*. We employed a monoclonal antibody directed against acetylated α-tubulin, which is predominantly found in the axoneme of mature neurons.

Marker gene analysis had indicated that the first differentiating RGCs appear at 35 hpf (Fig. 3F). At this stage acetylated α-tubulin staining showed very few axons leaving the eye, with no obvious projections from the eye to the optic tectum (Fig. 4A,A′). In contrast to functional fish retinae, the few forming axons that were observed did not exit the retina at a single site (optic disc) but rather individually without any clear direction to their projections (Fig. 4A,A′, arrows). At 38 hpf, which is the peak of RGC marker expression (differentiation), some RGC axons formed a dispersed optic disc-like structure (Fig. 4B′, arrow). However, these axons remained in the area of the eye and did not form any structure resembling a projecting optic nerve. These short axon clusters did not extend beyond the eye and did not form any projections to the tectum at this or subsequent stages.

RGCs with short axons were initially formed (Fig. 4A-C) and transiently maintained. They varied in length (25-100 µm) and stretched only a small fraction of the distance to the optic tectum. At 86 hpf, the eyes had already degenerated and had sunk into the surrounding tissue. Even though the eye could not be seen from the outside, it was recognisable by condensed DAPI staining. Only very few isolated residual RGCs still showed short axons (Fig. 4D′, arrow). The axonal connections/protrusions observed at 35 hpf, 45 hpf and 86 hpf could only occasionally be seen and not in all embryos analysed (not shown). Interestingly, and in contrast to the situation in the retina, the number of neurons within the olfactory

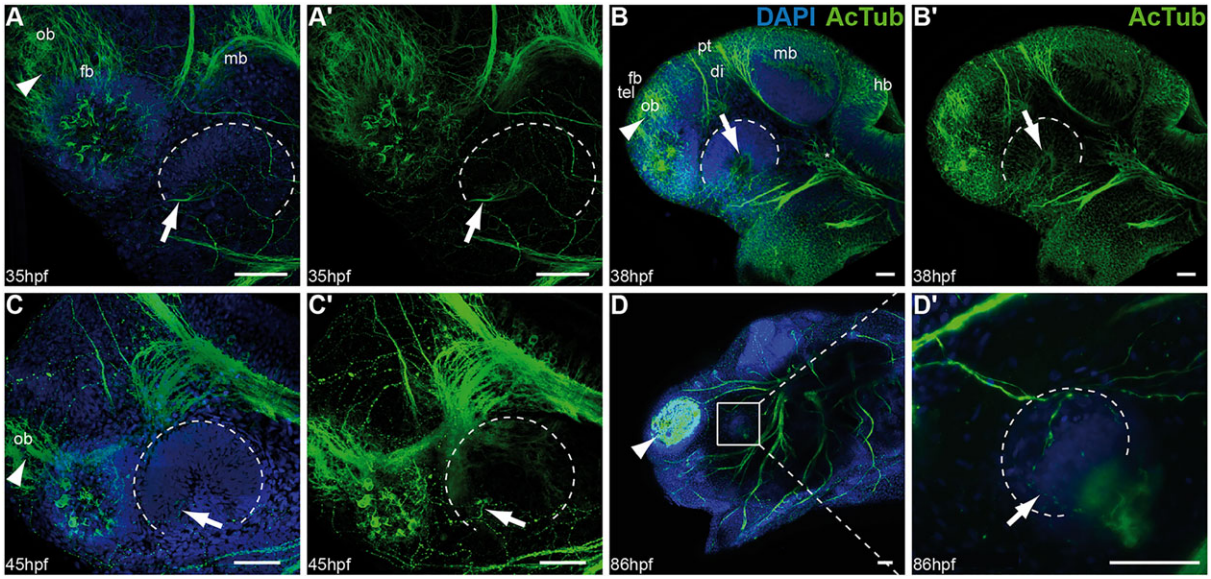

Fig. 4. Anatomy of the nervous system of *P. andruzzii*. Whole-mount immunostaining for acetylated α-tubulin (green) and staining with DAPI (blue). All embryos are in lateral view with anterior to the left. Images show maximum *z*-projections. At stage 35 hpf (A,A′) growing axons connecting hindbrain, midbrain, forebrain and olfactory system become apparent; additionally, thin axons exiting the retina are detected (arrows). More extensive staining of the retina was observed at stage 38 hpf (B,B′). The few stained RGC axon bundles are likely to represent a widened optic disc (arrows). At 45 hpf (C,C′) only two neighbouring retinal cells show axonal protrusions (arrows), while the neurons of the olfactory system had grown in number. At 86 hpf (D,D′), the eye had degenerated and sunk into the surrounding tissue. Only a few residual neurons in the retina showed the α-tubulin signal, while the olfactory bulb had grown further. D′ is a magnification of D showing retinal staining and thin axons protruding from the eye and seemingly projecting further (arrow). Retinae are encircled by dashed lines. di, diencephalon; fb, forebrain; hb, hindbrain; mb, midbrain; ob, olfactory bulb (arrowheads); pt, pretectum; tel, telencephalon. Scale bars: 50 µm.

Development (2015) 142, 743-752 doi:10.1242/dev.114629

bulb increased massively in the first 5 days of embryogenesis (Fig. 4A-D, arrowheads).

Degeneration of the cavefish eye is accompanied by activated Caspase3 expression

Active cell death by apoptosis is a key feature of eye degeneration in *Astyanax* and we observed autolytic vacuoles in the retina of *Phreatichthys* (Berti et al., 2001). Immunostaining on whole-mount preparations and on cryosections with an antibody directed against activated Caspase3 was performed to investigate the timing and distribution of apoptotic cells in *Phreatichthys* relative to the block in retinal differentiation.

Prior to the onset of RGC differentiation (31 hpf, Fig. 3A), only a few apoptotic cells were detected in the eye, whereas there was a marked focus of activated Caspase3-positive cells in the olfactory bulb (Fig. 5A, arrow). With the onset of RGC terminal differentiation at 35 hpf, a marked increase in retinal apoptosis was detected (Fig. 5B). The increase became obvious in comparison to the olfactory bulb (Fig. 5A, arrow). Concomitant with the progression of *atoh7* expression preceding RGC differentiation we observed an increase in retinal apoptosis, which appeared to spread from the centre of the retina to its margins (Fig. 5C-E). This is well represented in serial sections (Fig. 5D,E), in which active Caspase3 is preferentially detected at the periphery (Fig. 5E). Here, autolytic vacuoles form (Fig. 5E, arrows) that consist of dead cell material only. The predominant localisation of apoptotic activity to the neuroretina was independently confirmed by TUNEL staining (Fig. 5F,G). Similar to active Caspase3, DNA fragmentation as a hallmark of apoptosis was detected in the central region of the retina (compare Fig. 5C′ with 5F,G). Interestingly, and in contrast to *Astyanax*, only very few apoptotic cells were present in the lens at any of the stages analysed.

DISCUSSION

We have studied eye development and degeneration in the Somalian cavefish *Phreatichthys* to address whether evolution has targeted a similar ‘developmental soft spot’ in distantly related cavefish, or, alternatively, if independent steps in eye development and maintenance were targeted. We reveal that, in contrast to *Astyanax*, the eye primordium in *Phreatichthys* is morphologically unaltered and key factors involved in early eye development are expressed in patterns highly reminiscent of their orthologues in eyed teleosts. However, the key step in retina formation, which is the differentiation of neuronal cell types, failed to proceed beyond the birth of the first retinal neurons, the RGCs. These neither fully established nor maintained (even partial) functionality. Concomitant with the birth of RGCs, we detected a wave of apoptosis following the wave of RGC initiation. Consistently, only a few retinal neurons extending short axons formed in the prospective ganglion cell layer of the retina. Even though an optic disc-like structure was established transiently, the few surviving RGCs failed to establish connections with the optic tectum, which, similar to the retina, was severely affected by apoptosis.

The early eye field is established and patterned in *P. andruzzii*

It has been suggested that in *Astyanax* the patterning of the eye field is already affected (Yamamoto et al., 2004). Prior to the evagination of the optic vesicles, the eye field is defined at the anterior end of the neuroectoderm. It is patterned in a proximodistal direction by signals emanating from the ventral midline. In particular, the secreted signalling molecule Shh has been demonstrated to promote proximal cell fates (as indicated by *pax2* expression) and at the same time to repress distal fates, in particular *pax6* expression (Macdonald et al., 1995). This aspect of early patterning seems

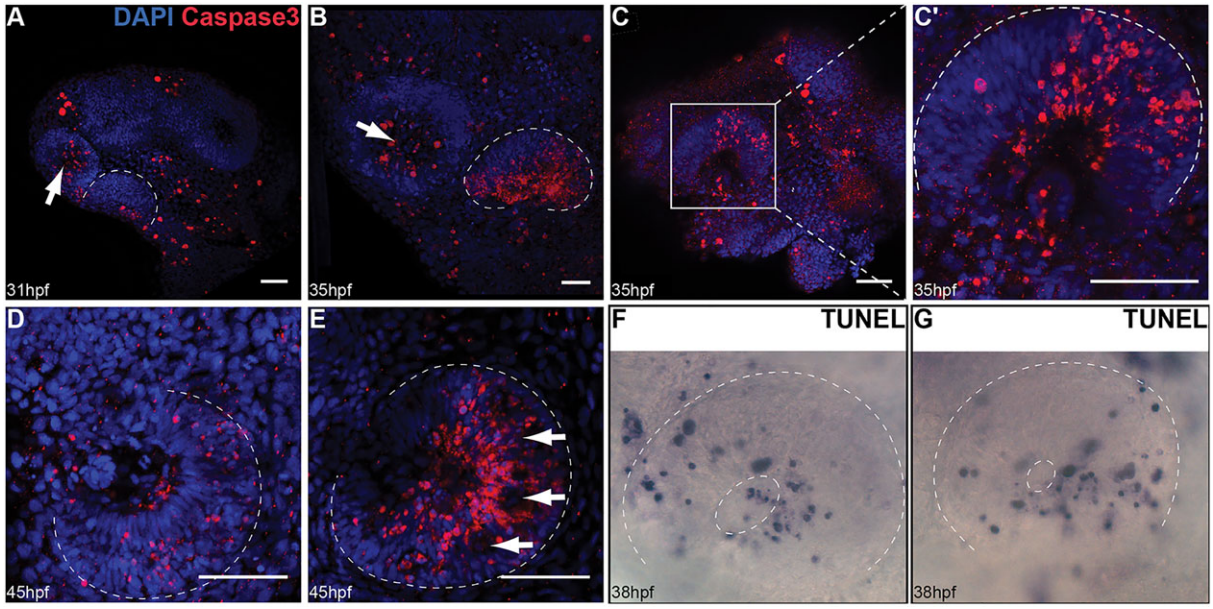

Fig. 5. Distribution of apoptotic cells in *P. andruzzii* embryos. (A-E) Immunostaining for activated Caspase3 (red) and DAPI staining (blue). (A-C′) Lateral view of whole-mount embryo with anterior to the left and dorsal up; (D,E) cryosections. Caspase3 staining was detected in the embryo at 31 hpf (A), most prominently in the olfactory bulb (arrow), but only faintly in the retina. At 35 hpf (B), prominent apoptosis is detected in the retina and in the olfactory bulb (arrow) (maximum projections in A,B). Optical sections indicate that apoptosis is initiated centrally at 35 hpf (C, at the level of the lens). (C′) Higher magnification of C showing that retinal apoptosis had not yet reached the periphery of the eye. At 45 hpf (D at central level; E at peripheral level), extensive apoptosis is detected throughout the entire retina. Higher densities of activated Caspase3-positive cells were detected in rosettes surrounding the autolytic vesicles (arrows). Whole-mount images of TUNEL-stained eyes of two specimens (F,G) at 38 hpf. Staining resembled the activated Caspase3 pattern. Retinae are encircled by dashed lines. Scale bars: 50 µm.

Development (2015) 142, 743-752 doi:10.1242/dev.114629

affected in *Astyanax*, where enhanced expression of midline *shh* (Yamamoto et al., 2004) results in the repression of Pax6 in the distal eye field leading to a reduction in the size of the optic primordia from early stages onward (Rétaux et al., 2008; Soares et al., 2004).

Our analyses in *P. andruzzii* indicate that there is no such enhanced activity of Shh in the midline. We found neither an expanded *shh* expression domain during the establishment of the eye field nor enhanced *shh* activity as indicated by an enhanced proximal *pax2* expression at the expense of distal *pax6* expression or by shifts in the expression of other factors downstream of *shh* (e.g. *nkx2.1*, *fgf8*). In contrast to *Astyanax*, *Phreatichthys pax2* and *pax6* are expressed in a pattern comparable to that in other teleost species. This apparently normal expression of proximal *pax2* and distal *pax6* serves as an internal control for correct early patterning, even in the absence of a comparison with a surface sister species. Thus, evolution has apparently targeted different developmental modules in *Astyanax* and in *Phreatichthys*, both resulting in the absence of eyes.

Neuroretinal differentiation is initiated but does not proceed

Concomitant with optic cup formation, the differentiation of the neural retina proceeds. As in all vertebrates, RPCs of teleosts follow a stereotypic order of differentiation into retinal cell types. Differentiation in *P. andruzzii* is initiated in central progenitors and expands radially. However, it never reaches the periphery, where a second reservoir of stem cells in the CMZ contributes to the growing retina. Our analyses indicate that in *Phreatichthys* the eyes are not maintained due to a failure of progenitor cells to terminally differentiate, and thus to follow the continuous and stereotypic formation of mature retinal cell types. Failing to terminally differentiate, RPCs are eliminated by a wave of progressive apoptosis that follows the RGC initiation as indicated by *atoh7*, one of the first differentiation factors expressed in the retina and which marks RPCs destined to become RGCs in their final mitosis (Kay et al., 2001; Mu et al., 2005). Although the initial step of RGC differentiation is taken, markers for postmitotic, differentiated RGCs [*isl1* and *pou4f2* (Prasov and Glaser, 2012)] are only transiently expressed. Pou4f2 has been specifically attributed to the establishment of axonal projections from RGCs (Jain et al., 2012). Consistently, only a few RGC axons form transiently and these fail to project towards the optic tectum.

Our data point to a block in differentiation after the appearance of RGCs in the inner layer of the retina (Fig. 6). The retina develops normally at the onset, but subsequent cell types are not generated and thereby overall eye development arrests.

Eye regression is more severe in *Phreatichthys* than in other cavefish models (Berti et al., 2001; Jeffery, 2009; Meng et al., 2013; Wilkens, 2007), correlating well with the longer separation from its surface ancestors (about two million years ago). However, there is no correlation between the time of separation and the developmental module tagged by different cave species, as indicated by an early module targeted in *Astyanax* (young cavefish), whereas a late differentiation module was affected in the ancient cavefish *Phreatichthys*.

These scenarios are underlined by the fact that *atoh7* is expressed only transiently in zebrafish and is not found in mature RGCs. The role of early Atoh7 expression in zebrafish is to confer progenitors with the competence to differentiate towards RGCs. The late expression of *atoh7* in *Phreatichthys* and the absence of later cell types support the hypothesis that RGCs do not differentiate properly and the remaining progenitors are not competent to give rise to other cell types.

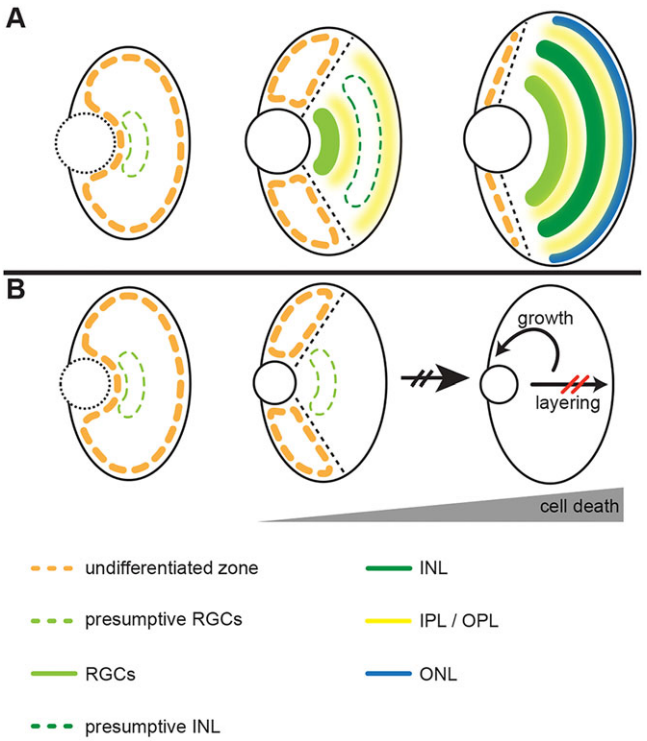

Fig. 6. Eye development of *P. andruzzii* ceases during RGC differentiation. (A) Normal eye development in known fish models. The neuroretina is initially undifferentiated, but eventually differentiates from the centre to the periphery in a stereotypic fashion. RGCs are the first-born cells in a layer close to the lens, followed by six more cell types including the last-born Müller glia cells. Each cell type will be located within its corresponding retinal layer, while the undifferentiated area becomes more restricted with time and eventually forms the CMZ, contributing to growth. (B) By contrast, eye development in *P. andruzzii* ceases while RGCs become specified and no further cell types or subsequent layering can be detected. Concurrent with the onset of differentiation, apoptosis is initiated and spreads over the neuroretina leading to full eye degeneration. RGCs, retinal ganglion cells; INL, inner nuclear layer; IPL, inner plexiform layer; OPL, outer plexiform layer; ONL, outer nuclear layer.

Strikingly, none of the cell types that follow on from RGCs in the birth order in the vertebrate retina could be detected. Rather than observing a secondary wave of differentiation with markers for the inner nuclear layer, namely *barhl2* [amacrine cells (Mo et al., 2004; Schuhmacher et al., 2011)] and *vsx1* [bipolar cells (Passini et al., 1997)], we revealed a wave of apoptosis following the initiation of RGC differentiation. This is in striking contrast to the situation in *Astyanax* (Alunni et al., 2007), in which marker gene expression indicates a terminal differentiation of different retinal neurons.

It has been suggested that apoptosis is a key player in cavefish eye degeneration (Berti et al., 2001; Jeffery and Martasian, 1998). We show that, in *Phreatichthys*, Caspase3 activity is high throughout the entire head during early stages. Although there was some variability early on, we consistently observed increased apoptosis levels in the retina from 35 hpf onwards. In contrast to *Astyanax*, where cell death is first detected in the lens and subsequently in autolytic rosettes in the retina, we did not observe enhanced apoptosis in the lens. It cannot be excluded that the shrinking lens is affecting the retina. Conversely, the failure to differentiate retinal cell types could also impact the maintenance of the lens. Eye degeneration can also be lens independent, as in the Chinese cavefish *Sinocyclocheilus* (Meng et al., 2013).

Development (2015) 142, 743-752 doi:10.1242/dev.114629

We hypothesize that, in response to the dysregulated differentiation of RPCs and subsequent cell types, retinal apoptosis is initiated to protect the structure against the overproliferation of aberrant cells. Thus, we speculate that a simple differentiation block building on intrinsic control mechanisms elegantly eliminates the *Phreatichthys* retina.

Conclusions

Our studies in *Phreatichthys* shed light on an evolutionary strategy to eradicate an organ by building on endogenous checkpoints for differentiation control and their measures to eliminate cells that fail to differentiate according to plan. It is striking that evolution has apparently followed different strategies in different species to eventually eliminate the same organ. By characterising these different evolutionary strategies that have eradicated the eye, insight gained from the study of additional cavefish species has the exciting potential to identify the normal developmental building blocks that establish and maintain the retina.

MATERIALS AND METHODS

Fixation of embryos

P. andruzzii embryos were raised at 28°C as previously described (Berti et al., 2001) and fixed at different stages with 4% paraformaldehyde (PFA) pH 7.2 in 1× PTW [phosphate-buffered saline (PBS) containing 0.1% Tween 20, pH 7.3] for 24 h at 4°C. Then, they were transferred to 100% methanol and stored at −20°C. The animal handling procedures and research protocols were approved by the Institutional Animal Care and Use Committee of the University of Ferrara (Italy) and by the Italian Ministry of Health. All fish housing and care conformed to directive 2010/63/UE on the protection of animals used for scientific purposes.

Cloning of partial cDNAs

Total RNA from *P. andruzzii* embryos was extracted using TRIzol Reagent (Life Technologies). TURBO DNAse (Ambion) was used to remove residual DNA, and isolated RNA was purified with an RNeasy Mini Kit (Qiagen). The subsequent cDNA synthesis was performed with a Maxima First Strand cDNA Synthesis Kit (Thermo Scientific). Genomic DNA was isolated with conventional Phenol/Chloroform/Isoamyl alcohol (PCI; Carl Roth) extraction. Reactions were performed with the Qiagen HotStar Taq PCR Kit. Each reaction (50 µl) contained 1× reaction buffer, 1× Q-Solution, 200 µM each dATP, dTTP, dGTP and dCTP, 0.5 µM each primer, 100 µM $MgCl_2$, 1% DMSO, 50 ng cDNA/genomic DNA and 0.02 U/µl HotStar Taq DNA polymerase. PCR employed the following cycling conditions: initial heat activation at 95°C for 15 min; ten cycles of 95°C for 30 s, 45°C for 1 min then +0.5°C/cycle, 72°C for 1 min; ten cycles of 95°C for 30 s, 52°C for 1 min, 72°C for 1 min; ten cycles of 95°C for 30 s, 55°C for 1 min then +0.5°C/cycle, 72°C for 1 min; five cycles of 95°C for 30 s, 62°C for 1 min, 72°C for 1 min; with final extension of 10 min at 72°C and cooling to 4°C for 5 min. PCR products were cloned into the pGEM-T Easy vector (Promega) following the supplier's instructions. The validity of the respective cDNAs was confirmed by sequence analysis. For primer sequences see supplementary material Table S1. Sequences were submitted to GenBank (NCBI): *PA_atoh7* (KJ867022), *PA_barhl2* (KJ867023), *PA_pou4f2* (KJ867024), *PA_pax6* (KJ867025), *PA_rx2* (KJ867026), *PA_rx3* (KJ867027), *PA_shh* (KJ867028), *PA_six3a* (KJ867029), *PA_sox2* (KJ867030), *PA_nr2e1* (KJ867031), *PA_vsx1* (KJ867032), *PA_isl1* (KJ867033), *PA_crx* (KJ867034), *PA_opsin* (KJ867035), *PA_rhodopsin* (KJ867036), *PA_fgf8* (KP125521), *PA_nkx2.1* (KP125522), *PA_pax2.1* (KP125523).

Generation of DIG-labelled ribonucleotide probes

Plasmid DNA containing the respective inserts was linearised and transcribed with SP6 or T7 RNA polymerase (Roche) in the presence of DIG-labelled dUTP (Roche, 11209256910) according to the manufacturer's instructions.

Whole-mount *in situ* hybridisation

In situ hybridisation (ISH) protocols are based on a protocol for single-colour ISH in zebrafish (Thisse and Thisse, 2008). Staining employed 4-nitroblue tetrazolium chloride (NBT) and 5-bromo-4-chloro-3-indolylphosphate (BCIP) from Roche.

Vibratome sectioning and imaging

Embryos were embedded in 1.5 ml gelatin albumin [PBS containing 0.5% gelatin, 30% albumin from bovine serum Cohn fraction 5 (Sigma)] and solidified with 105 µl glutaraldehyde. Transverse sections (30 µm) were cut with a VT1000 S vibrating blade microtome (Leica) and mounted on microscope slides with Mowiol [1 g/ml glycerin, 0.4 g/ml Mowiol 4-88 (Carl Roth), 0.4 M Tris-HCl pH 8.5, 25 mg/ml DABCO (Sigma-Aldrich)]. Embryos at 10 hpf and 19 hpf were dissected from the yolk and mounted in PTW containing 50% glycerol on slides.

Cryosectioning and immunohistochemistry

After overnight fixation at 4°C, embryos were washed five times for 5 min each in PTW and then permeabilised with 100% acetone for 10 min at −20°C. Embryos were transferred back to PTW, washed and cryoprotected with 1× PTW containing 30% sucrose for 24 h at 4°C. Embryos were mounted in polyethylene embedding moulds (Polyscience) and sucrose was removed completely. The specimens were embedded in Tissue-Tek O.C.T. Compound (Sakura). Sections (16-30 µm) were cut on a CM3050S cryostat (Leica) and mounted on SuperFrost Plus slides (Thermo Scientific).

After at least 2 h of drying at room temperature (RT), sections were rehydrated with PTW and blocked with 10% serum blocking buffer (10% sheep serum in PTW) for 1 h on a shaker at RT. Blocking buffer was removed and slides were washed four times for 5 min each with PTW. Primary antibodies were diluted in 1% serum buffer (1% sheep serum in PTW) and pipetted onto the sections, which were then covered with Parafilm and stored in a humid atmosphere in a closed box overnight at 4°C. The slides were washed four times for 30 min each with PTW and then incubated with secondary antibody diluted in 1% serum buffer overnight at 4°C. For Caspase3 staining, monoclonal anti-rabbit activated Caspase3 antibody (Abcam, ab13847) was used at 1:300. Anti-mouse PCNA antibody (Millipore, CBL407) was diluted 1:100. The secondary antibodies Alexa 488 anti-mouse and Alexa 594 anti-rabbit (Life Technologies) were used at 1:200 and 1:1000, respectively. After antibody staining, slides were incubated with PTW containing 1:1000 DAPI (Sigma; stock concentration 500 µg/ml) for 15 min at RT, then washed with PTW, mounted with 50% glycerol and covered with a coverslip.

Whole-mount immunohistochemistry

Embryos were stored in 100% methanol and rehydrated into PTW in successive washings. Embryos were blocked with 10% serum blocking buffer in 2 ml reaction tubes for 1.5 h on a shaker at RT. Blocking buffer was removed and embryos were washed four times for 5 min each with PTW. Embryos were then transferred to 0.5 ml reaction tubes and 300 µl of antibody solution was added. Primary antibodies were diluted in 1% serum buffer and incubated on a rotator at 4°C overnight. Embryos were then washed four times for 30 min each with PTW in 2 ml tubes and incubated with secondary antibody diluted in 1% serum buffer overnight at 4°C in 0.5 ml tubes. For Caspase3 staining, monoclonal anti-rabbit activated Caspase3 antibody (Abcam) specific for apoptotic cells was used at 1:300. Monoclonal anti-mouse acetylated α-tubulin antibody (Sigma Aldrich, T6793) was diluted 1:500. The secondary antibodies Alexa 488 anti-mouse and Alexa 594 anti-rabbit (Life Technologies) were used at 1:1000; DAPI (Sigma-Aldrich; 1:500) was added together with the secondary antibodies. Subsequently, embryos were washed with PTW, mounted laterally with 1% low-melting agarose in a glass-bottom dish and imaged by confocal microscopy.

Whole-mount TUNEL staining

Embryos were fixed, stored and proteinase K-treated according to the ISH protocol (see above). TUNEL assay was carried out with *In Situ* Cell Death Detection Kit, AP (Roche) according to the manufacturer's instructions.

Development (2015) 142, 743-752 doi:10.1242/dev.114629

Imaging

Fluorescent samples were imaged using a Leica SPE confocal microscope, 20× water-immersion objective and Leica Application Suite (LAS) software. Alexa 488 was excited at 488 nm by argon laser, Alexa 594 by a 543 nm helium neon laser and DAPI by an UV laser at 405 nm. Emission was sensed at 500-550 nm for Alexa 488, 650-700 nm for Alexa 594 and 410-500 nm for DAPI. ISH and TUNEL stained samples were imaged with an Axio Imager M1 (Zeiss), differential interference contrast (DIC) channel and 10× or 20× objective, Zeiss AxioCam camera and AxioVision software. Images were processed using Adobe Photoshop CS4 and Adobe Illustrator CS4.

Acknowledgements

We acknowledge the entire J.W. department for critical discussion during the project and comments on the manuscript. We thank Elena Frigato for help with animal care and sampling. M.S. is a member of the HBIGS Graduate School for Life Sciences at Heidelberg University.

Competing interests

The authors declare no competing or financial interests.

Author contributions

L.-N.S. and J.W. initiated the project; L.-N.S., M.S. and J.W. planned the experiments in collaboration with C.B. and N.S.F.; L.-N.S. and M.S. performed all experiments and analysed the data together with J.W.; staged *Phreatichthys* embryos were provided by C.B.; M.S., L.-N.S. and J.W. wrote the manuscript with contributions from C.B. and N.S.F.

Funding

The project was supported by grants from the German Research Foundation (DFG) and the European Research Council (ERC) to J.W.

Supplementary material

Supplementary material available online at
http://dev.biologists.org/lookup/suppl/doi:10.1242/dev.114629/-/DC1

References

Agathocleous, M. and Harris, W. A. (2009). From progenitors to differentiated cells in the vertebrate retina. *Annu. Rev. Cell Dev. Biol.* **25**, 45-69.

Agathocleous, M., Iordanova, I., Willardsen, M. I., Xue, X. Y., Vetter, M. L., Harris, W. A. and Moore, K. B. (2009). A directional Wnt/beta-catenin-Sox2-proneural pathway regulates the transition from proliferation to differentiation in the Xenopus retina. *Development* **136**, 3289-3299.

Alunni, A., Menuet, A., Candal, E., Pénigault, J.-B., Jeffery, W. R. and Rétaux, S. (2007). Developmental mechanisms for retinal degeneration in the blind cavefish Astyanax mexicanus. *J. Comp. Neurol.* **505**, 221-233.

Berti, R., Durand, J. P., Becchi, S., Brizzi, R., Keller, N. and Ruffat, G. (2001). Eye degeneration in the blind cave-dwelling fish Phreatichthys andruzzii. *Can. J. Zool.* **79**, 1278-1285.

Besharse, J. C. and Brandon, R. A. (1974). Postembryonic eye degeneration in the troglobitic salamander Typhlotriton spelaeus. *J. Morphol.* **144**, 381-405.

Carl, M., Loosli, F. and Wittbrodt, J. (2002). Six3 inactivation reveals its essential role for the formation and patterning of the vertebrate eye. *Development* **129**, 4057-4063.

Cavallari, N., Frigato, E., Vallone, D., Fröhlich, N., Lopez-Olmeda, J. F., Foà, A., Berti, R., Sánchez-Vázquez, F. J., Bertolucci, C. and Foulkes, N. S. (2011). A blind circadian clock in cavefish reveals that opsins mediate peripheral clock photoreception. *PLoS Biol.* **9**, e1001142.

Centanin, L. and Wittbrodt, J. (2014). Retinal neurogenesis. *Development* **141**, 241-244.

Centanin, L., Hoeckendorf, B. and Wittbrodt, J. (2011). Fate restriction and multipotency in retinal stem cells. *Cell Stem Cell* **9**, 553-562.

Dezfuli, B. S., Capuano, S., Magosso, S., Giari, L. and Berti, R. (2009a). The lateral line system in larvae of the blind cyprinid cavefish, Phreatichthys andruzzii. *Anat. Rec. (Hoboken)* **292**, 423-430.

Dezfuli, B. S., Magosso, S., Simoni, E., Hills, K. and Berti, R. (2009b). Ultrastructure and distribution of superficial neuromasts of blind cavefish, Phreatichthys andruzzii, juveniles. *Microsc. Res. Tech.* **72**, 665-671.

Ekonomou, A., Kazanis, I., Malas, S., Wood, H., Alifragis, P., Denaxa, M., Karagogeos, D., Constanti, A., Lovell-Badge, R. and Episkopou, V. (2005). Neuronal migration and ventral subtype identity in the telencephalon depend on SOX1. *PLoS Biol.* **3**, e186.

Hecht, M. K., Wallace, B. and Wilkens, H. (1988). Evolution and genetics of epigean and cave Astyanax fasciatus (Characidae, Pisces): support for the neutral mutation theory. *Evol. Biol.* **23**, 271-367.

Hinaux, H., Pottin, K., Chalhoub, H., Père, S., Elipot, Y., Legendre, L. and Rétaux, S. (2011). A developmental staging table for Astyanax mexicanus surface fish and Pachón cavefish. *Zebrafish* **8**, 155-165.

Jain, V., Ravindran, E. and Dhingra, N. K. (2012). Differential expression of Brn3 transcription factors in intrinsically photosensitive retinal ganglion cells in mouse. *J. Comp. Neurol.* **520**, 742-755.

Jeffery, W. R. (2001). Cavefish as a model system in evolutionary developmental biology. *Dev. Biol.* **231**, 1-12.

Jeffery, W. R. (2009). Regressive evolution in Astyanax cavefish. *Annu. Rev. Genet.* **43**, 25-47.

Jeffery, W. R. and Martasian, D. P. (1998). Evolution of eye regression in the cavefish astyanax: apoptosis and the Pax-6 gene. *Integr. Comp. Biol.* **38**, 685-696.

Jusuf, P. R., Albadri, S., Paolini, A., Currie, P. D., Argenton, F., Higashijima, S.-i., Harris, W. A. and Poggi, L. (2012). Biasing amacrine subtypes in the Atoh7 lineage through expression of Barhl2. *J. Neurosci.* **32**, 13929-13944.

Kay, J. N., Finger-Baier, K. C., Roeser, T., Staub, W. and Baier, H. (2001). Retinal ganglion cell genesis requires lakritz, a zebrafish atonal homolog. *Neuron* **30**, 725-736.

Kay, J. N., Link, B. A. and Baier, H. (2005). Staggered cell-intrinsic timing of ath5 expression underlies the wave of ganglion cell neurogenesis in the zebrafish retina. *Development* **132**, 2573-2585.

Lagutin, O. V., Zhu, C. C., Kobayashi, D., Topczewski, J., Shimamura, K., Puelles, L., Russell, H. R. C., McKinnon, P. J., Solnica-Krezel, L. and Oliver, G. (2003). Six3 repression of Wnt signaling in the anterior neuroectoderm is essential for vertebrate forebrain development. *Genes Dev.* **17**, 368-379.

Loosli, F., Winkler, S. and Wittbrodt, J. (1999). Six3 overexpression initiates the formation of ectopic retina. *Genes Dev.* **13**, 649-654.

Loosli, F., Winkler, S., Burgtorf, C., Wurmbach, E., Ansorge, W., Henrich, T., Grabher, C., Arendt, D., Carl, M., Krone, A. et al. (2001). Medaka eyeless is the key factor linking retinal determination and eye growth. *Development* **128**, 4035-4044.

Loosli, F., Staub, W., Finger-Baier, K. C., Ober, E. A., Verkade, H., Wittbrodt, J. and Baier, H. (2003). Loss of eyes in zebrafish caused by mutation of chokh/rx3. *EMBO Rep.* **4**, 894-899.

Macdonald, R., Barth, K., Xu, Q., Holder, N., Mikkola, I. and Wilson, S. W. (1995). Midline signalling is required for Pax gene regulation and patterning of the eyes. *Development* **121**, 3267-3278.

Mathers, P. H., Grinberg, A., Mahon, K. A. and Jamrich, M. (1997). The Rx homeobox gene is essential for vertebrate eye development. *Nature* **387**, 603-607.

Meng, F., Braasch, I., Phillips, J. B., Lin, X., Titus, T., Zhang, C. and Postlethwait, J. H. (2013). Evolution of the eye transcriptome under constant darkness in Sinocyclocheilus cavefish. *Mol. Biol. Evol.* **30**, 1527-1543.

Menuet, A., Alunni, A., Joly, J.-S., Jeffery, W. R. and Rétaux, S. (2007). Expanded expression of Sonic Hedgehog in Astyanax cavefish: multiple consequences on forebrain development and evolution. *Development* **134**, 845-855.

Mo, Z., Li, S., Yang, X. and Xiang, M. (2004). Role of the Barhl2 homeobox gene in the specification of glycinergic amacrine cells. *Development* **131**, 1607-1618.

Moshiri, A., Gonzalez, E., Tagawa, K., Maeda, H., Wang, M., Frishman, L. J. and Wang, S. W. (2008). Near complete loss of retinal ganglion cells in the math5/brn3b double knockout elicits severe reductions of other cell types during retinal development. *Dev. Biol.* **316**, 214-227.

Mu, X., Fu, X., Sun, H., Beremand, P. D., Thomas, T. L. and Klein, W. H. (2005). A gene network downstream of transcription factor Math5 regulates retinal progenitor cell competence and ganglion cell fate. *Dev. Biol.* **280**, 467-481.

Mu, X., Fu, X., Beremand, P. D., Thomas, T. L. and Klein, W. H. (2008). Gene-regulation logic in retinal ganglion cell development: Isl1 defines a critical branch distinct from but overlapping with Pou4f2. *Proc. Natl. Acad. Sci. USA* **105**, 6942-6947.

Passini, M. A., Levine, E. M., Canger, A. K., Raymond, P. A. and Schechter, N. (1997). Vsx-1 and Vsx-2: differential expression of two paired-like homeobox genes during zebrafish and goldfish retinogenesis. *J. Comp. Neurol.* **388**, 495-505.

Pipan, T. and Culver, D. C. (2012). Convergence and divergence in the subterranean realm: a reassessment. *Biol. J. Linn. Soc.* **107**, 1-14.

Pottin, K., Hinaux, H. and Rétaux, S. (2011). Restoring eye size in Astyanax mexicanus blind cavefish embryos through modulation of the Shh and Fgf8 forebrain organising centres. *Development* **138**, 2467-2476.

Prasov, L. and Glaser, T. (2012). Dynamic expression of ganglion cell markers in retinal progenitors during the terminal cell cycle. *Mol. Cell. Neurosci.* **50**, 160-168.

Protas, M. and Jeffery, W. R. (2012). Evolution and development in cave animals: from fish to crustaceans. *Wiley Interdiscip. Rev. Dev. Biol.* **1**, 823-845.

Rétaux, S., Pottin, K. and Alunni, A. (2008). Shh and forebrain evolution in the blind cavefish Astyanax mexicanus. *Biol. Cell* **100**, 139-147.

Rohner, N., Jarosz, D. F., Kowalko, J. E., Yoshizawa, M., Jeffery, W. R., Borowsky, R. L., Lindquist, S. and Tabin, C. J. (2013). Cryptic variation in morphological evolution: HSP90 as a capacitor for loss of eyes in cavefish. *Science* **342**, 1372-1375.

Schuhmacher, L.-N., Albadri, S., Ramialison, M. and Poggi, L. (2011). Evolutionary relationships and diversification of barhl genes within retinal cell lineages. *BMC Evol. Biol.* **11**, 340.

Development (2015) 142, 743-752 doi:10.1242/dev.114629

Soares, D., Yamamoto, Y., Strickler, A. G. and Jeffery, W. R. (2004). The lens has a specific influence on optic nerve and tectum development in the blind cavefish Astyanax. *Dev. Neurosci.* **26**, 308-317.

Strickler, A. G., Yamamoto, Y. and Jeffery, W. R. (2007). The lens controls cell survival in the retina: evidence from the blind cavefish Astyanax. *Dev. Biol.* **311**, 512-523.

Thisse, C. and Thisse, B. (2008). High-resolution in situ hybridization to whole-mount zebrafish embryos. *Nat. Protoc.* **3**, 59-69.

Walther, C. and Gruss, P. (1991). Pax-6, a murine paired box gene, is expressed in the developing CNS. *Development* **113**, 1435-1449.

Wilkens, H. (2007). Regressive evolution: ontogeny and genetics of cavefish eye rudimentation. *Biol. J. Linn. Soc.* **92**, 287-296.

Wilkens, H. (2011). Variability and loss of functionless traits in cave animals. Reply to Jeffery (2010). *Heredity* **106**, 707-708.

Yamamoto, Y. (2000). Central role for the lens in cave fish eye degeneration. *Science* **289**, 631-633.

Yamamoto, Y., Stock, D. W. and Jeffery, W. R. (2004). Hedgehog signalling controls eye degeneration in blind cavefish. *Nature* **431**, 844-847.

Yamamoto, Y., Byerly, M. S., Jackman, W. R. and Jeffery, W. R. (2009). Pleiotropic functions of embryonic sonic hedgehog expression link jaw and taste bud amplification with eye loss during cavefish evolution. *Dev. Biol.* **330**, 200-211.

Zaghloul, N. A. and Moody, S. A. (2007). Alterations of rx1 and pax6 expression levels at neural plate stages differentially affect the production of retinal cell types and maintenance of retinal stem cell qualities. *Dev. Biol.* **306**, 222-240.

Zuber, M. E., Gestri, G., Viczian, A. S., Barsacchi, G. and Harris, W. A. (2003). Specification of the vertebrate eye by a network of eye field transcription factors. *Development* **130**, 5155-5167.